https://doi.org/10.48048/tis.2024.7059

The Role of Annealing Treatment on the Morphological Evolution and Swelling of ZnPc Layer on A QCM Sensor

Masruroh*, Dionysius J. D. H. Santjojo, Gancang Saroja, Tyas N. Zafirah and Setyawan P. Sakti

Department of Physics, Faculty of Mathematics and Natural Sciences, Brawijaya University, Indonesia

(*Corresponding author's e-mail: ruroh@ub.ac.id)

Received: 8 May 2023, Revised: 20 June 2023, Accepted: 23 June 2023, Published: 1 August 2023

Abstract

Morphological evolution and swelling were observed in the zinc phthalocyanine (ZnPc) layer on a quartz crystal microbalance (QCM) sensor treated with annealing. The morphology affects the swelling during analyte injection. The swelling effect can shorten the QCM sensor recovery time. The ZnPc layer was deposited on the surface of the polystyrene/QCM by evaporation technique. The annealing process was conducted for 1 h at 3 temperature variations: 100, 150, and 220 °C. The swelling experiments were carried out by injecting PBS and Tris-HCl solution into the layer. The surface morphology characterization of ZnPc was observed using an SEM/EDX before and after swelling. The morphological evolution from the network into fibers change to disentangled of the ZnPc molecular chain and broke into a shorter fiber. The diffractogram revealed a monoclinic phase for the samples annealed at 100 and 150 °C. On the other hand, the sample annealed at 220 °C showed a triclinic phase. The formation of ZnPc crystal confirms the disordering structure leading to the morphology change. Further, the ZnPc fibers swell after the injection of PBS and Tris-HCl. Tris-HCl injection at high temperature annealing (220 °C) resulted in fiber tattering. Investigations on diffusion mechanisms were conducted by measuring the change in frequency. The ionic strength of the solutions controlled the diffusion. The PBS diffuses faster than the Tris-HCl into the ZnPc layer.

Keywords: Annealing treatment, Morphological evolution, ZnPc layer, Swelling, QCM

Introduction

Quartz Crystal Microbalance (QCM) is a mass sensor capable of measuring mass changes that occur on its surface based on shifts in the resonant frequency formulated by the Sauerbrey equation [1]. QCM is widely applied as a biosensor [2,3] and gas sensor [4-8]. Using the QCM as a sensor requires an active layer on its surface to increase the sensor response, selectivity, sensitivity, and measurement reproducibility of analytes. One of the most applied active sensor layers is made of polymeric materials. This polymer material was chosen because it has the advantages of high sensitivity, responding quickly to analytes, and operating at room temperature. This ability is mainly due to sorption interactions between the polymer layer and the analyte. Analytes that diffuse into the coating can cause swelling [9]. Besides the sorption alone, the swelling shifts the resonant frequency more significantly. This change affects the increase in sensor sensitivity.

Swelling is influenced by 2 factors, the layer and the liquid analyte properties [9]. The former properties include morphology [10-12], cross-linking [13,14], wettability [15] and layer thickness [16]. While the latter comprises the molecular weight of the analyte [17], the affinity between substrate-liquid [18], solution concentration [19], ionic strength [20], and layer polarity [15]. Besides, research conducted by Al-Anbakey 2013 showed that the swelling effect in polyacrylic acid (PAA) is controlled by temperature [21]. The swelling is caused by the internal energy and entropy of the PAA layer, which increases in proportion to the increase in temperature, encouraging the diffusion of more and more analytes.

Recently, conductive polymers such as metal phthalocyanine (MPc) have received much attention because of considerable variation in molecular structure [22-24]. Phthalocyanine (Pc) is an organic compound that can be modified by replacing 2 hydrogen atoms in the center with metal atoms or other compounds [23]. Replacing hydrogen atoms with metal atoms will produce its derivative compounds called metal phthalocyanine (MPc). The widely used metal types are transitional metals, such as *Zn*, *Cu*, *Fe*, *Co*, and *Ni* [24,25]. Zinc phthalocyanine (ZnPc) is 1 type of *Zn* metal cation in its central cavity [26]. ZnPc comprises a phthalocyanine ($C_{32}H_{16}N_8$) ring with a transition metal core (*Zn*). All interactions π and core-

shell in the phthalocyanine branches are dominated by Van Der Waals bonds, making these molecules easily interact with liquid analyte molecules [27,28]. In addition, ZnPc molecules can also trigger the emergence of physical interactions such as π and π^* orbitals [29]. These advantages make the ZnPc a suitable biosensor active layer [30-32].

Our previous research showed the swelling effect observed in the CuPc using a quartz crystal microbalance (QCM) sensor layer injected with a liquid analyte [10,33]. The swelling effect observed by the injection of PBS and Tris-Cl increases the analyte absorption and the change in the QCM oscillation frequency. The pattern of continuous frequency changes indicates the diffusion of the liquid molecules into a thin layer on the surface of the QCM. The swelling ability is required to improve the sensor performance. This study observed the annealing effect on the morphology of the ZnPc layer and the swelling effects that occur by injecting with variations in the buffer type (PBS and Tris-CL). Observations were made through changes in the frequency of QCM sensor resonance due to the swelling effect.

Materials and methods

The polystyrene (PS) interlayer is deposited using a spin coating method on the surface of the QCM 10 MHz sensor with silver electrodes (purchased from PT Great Microtama). The PS interlayer layer increases the interaction between the QCM substrate and the thin layer of ZnPc. PS 192 g/mol obtained from Sigma Aldrich is dissolved in toluene solvents until a solution with a concentration of 6 % is obtained. The solution was dropped and spun on the QCM. The spinning was conducted for 60 s with a speed of 3,000 rpm. The PS layer was annealed at 200 °C for 1 h to evaporate the solvent and produce a smooth surface.

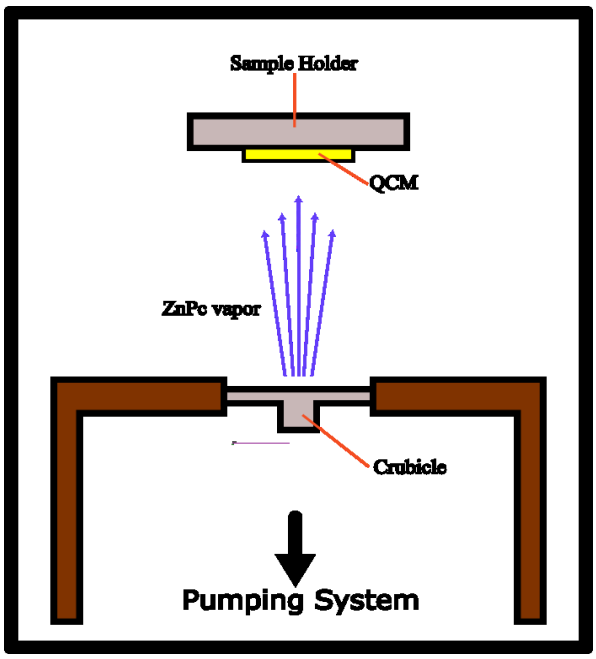

Figure 1 Vacuum thermal evaporation deposition system.

The deposition of ZnPc on the surface of the QCM sensor was carried out by the thermal evaporation method. The ZnPc powder (99 % purity) was purchased from Sigma Aldrich. A total of 5 mg of ZnPc powder is placed in a heating crucible 3 cm away from the surface of the QCM substrate. Then, the heater power supply voltage was raised gradually to 1.4 V. The ZnPc powder was evaporated for 5 min to form a thin layer on the surface of the QCM. **Figure 1** shows the vacuum evaporation system used in this study. The thin layer of ZnPc was then annealed for 1 h with 3 temperature variations, i.e., 100, 150, and 220 °C. The morphology of the annealed ZnPc layers was observed using a FESEM/EDX Quanta FEG 650 type. The X-ray Bragg-Brentano diffraction technique was used to determine the crystalline structure of the ZnPc. The measurements were conducted using a Panalytical X'Pert3 powder XRD system with Cu-Kα radiation (λ = 1.543Å). The diffracted beam was picked up using a high-sensitivity RTMS detector (X'Celerator Scientific) at 0.0167 degrees for 10.16 s per step. The diffraction peaks of ZnPc were compared with the standard JCPDS-ICDD tables (PDF 00-039-1882).

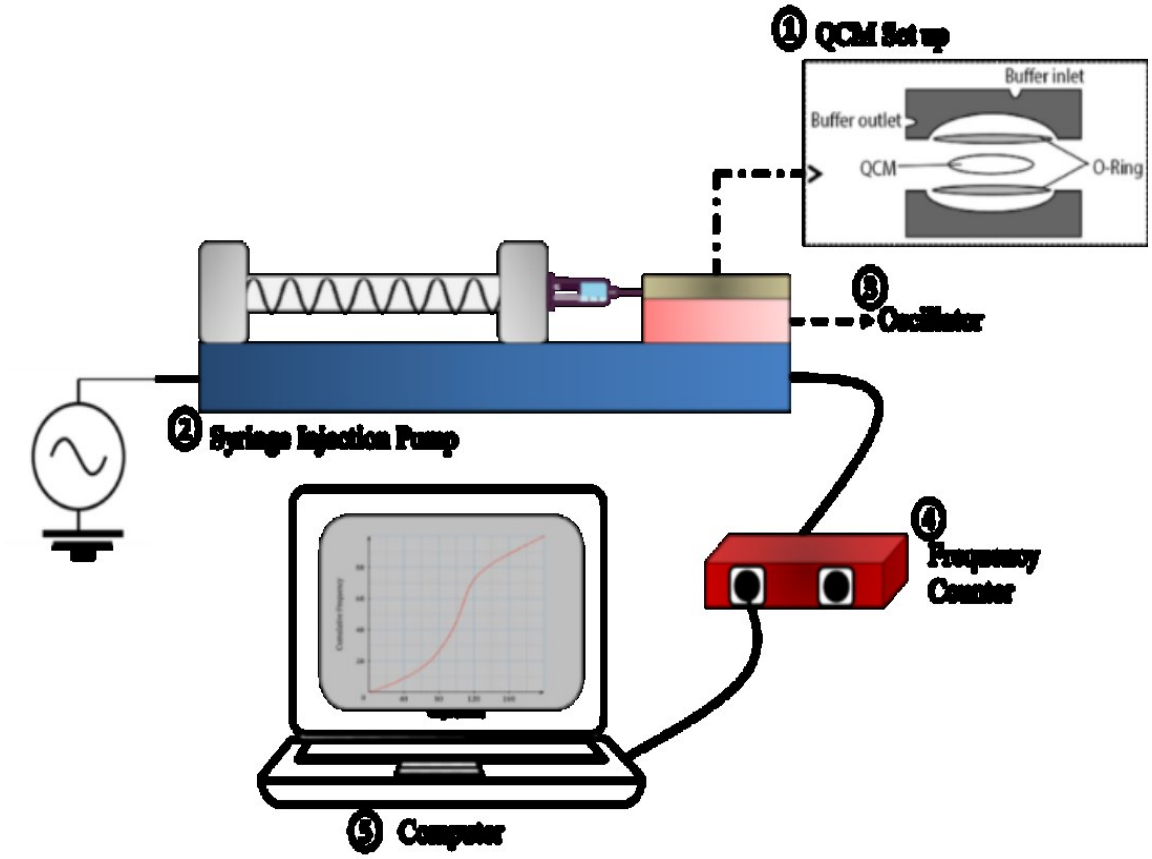

Figure 2 Experimental setup for investigating swelling of ZnPc on QCM sensor.

The above measurements (**Figure 2**) were also carried out to observe the swelling effect of the ZnPc layer by injecting 50 µl of 2 types of buffer solutions: phosphate buffered saline (PBS) pH 7.4 and ultrapure 1 M tris-hydrochloride buffer (tris-HCl) pH 7.5 a product of GIBCO made in the USA, for each variation of the annealing treatment. The study measured changes in the QCM frequency before and after the injection. The QCM was mounted in the cell and connected to an oscillator, as shown in **Figure 2**. A frequency counter was utilized to determine the resonance frequency of the QCM sensor. The QCM frequency measurement was carried out for an hour, which will then be plotted as a reference for the effect of annealing temperature on the swelling effect of the ZnPc layer on QCM.

Results and discussion

The annealing treatment of the ZnPc at various temperatures causes the gradual decomposition of its fibrous structure. The morphological structure of the ZnPc layer before annealing is the fibrous network, as shown in **Figure 3(a)**. There were no significant morphological changes for samples annealed at 100 °C (**Figure 3(b)**). The network was intact, but the fibers started to stretch, and the distance among them was wider. The fibers broke, and their tips were tapered at 150 °C of annealing. The fibers became much shorter and distributed in the layer. The phenomenon was more apparent in the samples annealed at 220 °C (**Figure 3(d)**). Furthermore, the space among them became broader and broader (**Figure 3(c)**). The morphological changes suggest that the fibers are homogenously distributed at higher annealing temperatures.

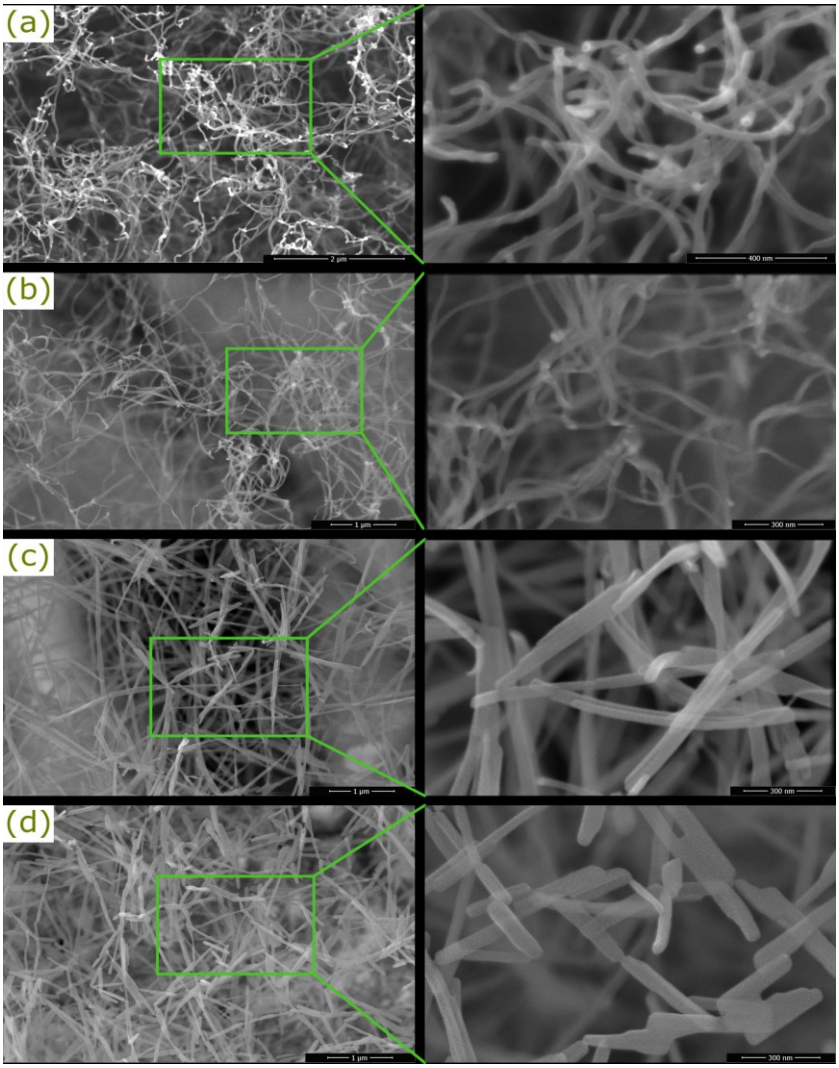

Figure 3 The morphology of ZnPc; (a) before annealing, (b) annealed at 100 °C, (c) annealed at 150 °C, and (d) annealed at 220 °C.

The microstructure ordering of ZnPc was investigated using the XRD, as shown in **Figure 4**. The untreated sample diffractogram shows only the SiO_2 substrate crystalline structure. The absence of the ZnPc peak indicates that the layer is amorphous. Crystallization of the ZnPc was observed at low angle $2\theta = 5$ ° to $2\theta = 11$ ° [26,29,34] The diffraction peaks after the annealing were found at $2\theta = 6.62$ °, $2\theta = 6.94$ ° and the weak reflection at $2\theta = 9.63$ °. The samples annealed at 100 and 150 °C exhibit a monoclinic phase. The phase is characterized by the peak at $2\theta = 6.94$ ° and $2\theta = 9.63$ ° related to the (200) and (202) plane, respectively. A decrease in the intensity value of the monoclinic phase in the (200) crystal plane occurs up to an annealing temperature of 150 °C. Higher temperature annealing resulted in phase transformation into triclinic, which can be confirmed with the (100) peak at $2\theta = 6.62$ ° [34]. The transformation indicates the disordering of the crystal, which trigger the morphological evolution.

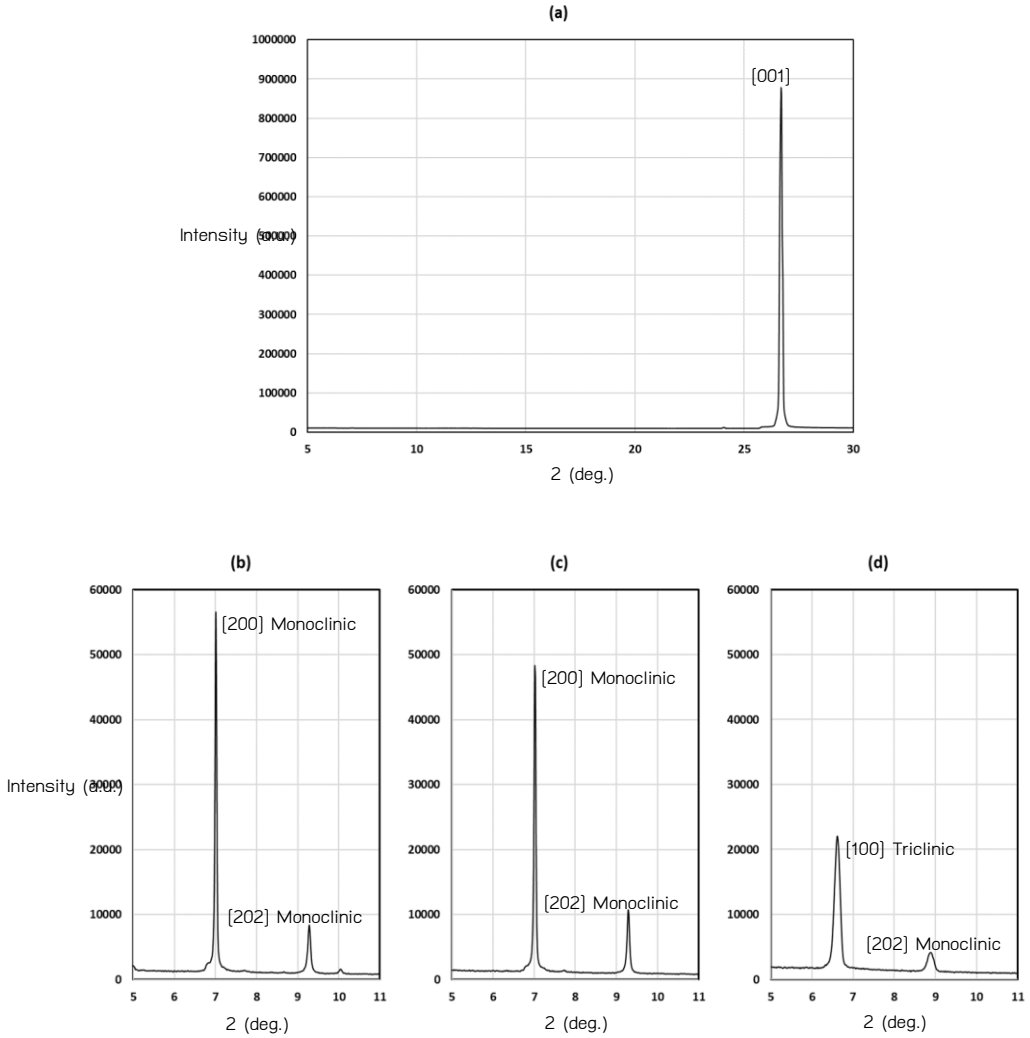

Figure 4 Diffractogram of ZnPc layer; (a) untreated, (b) annealed at 100 °C, (c) annealed at 150 °C, and (d) annealed at 220 °C.

The layer experiencing molecular stretching due to annealing is crucial in sensor analyte detection. The stretched layer increases porosity, which can also be the entrance of the analyte molecules to be absorbed into the ZnPc layer. This analyte molecule absorption is closely related to the swelling ability of the ZnPc layer. The swelling of the layer was studied by observing the surface morphology change and measuring changes in the QCM frequency after the injection of buffer solutions, i.e., PBS and Tris-HCl. The SEM images in **Figure 5** show the annealed ZnPc layer swelling after the injection of PBS and Tris-HCl. The observations also noticed the broadening of space among the fibers. Detailed studies on the slight change of the sample annealed at 100 °C reveal that limited interactions between the layer and the buffer caused only small diffusion into the fiber. The buffer solutions diffuse more in the samples annealed at 150 °C, indicated by the significant widening/swelling of the fibers. The ZnPc layer accommodates a larger driving force of the buffer molecules, pushing them into the fibers. Further broadening of inter-fiber space was also facilitated for these samples. An interesting phenomenon was observed for the samples annealed at 220 °C, where the SEM image shows extreme shortening and deformation of fibers due to the injection of PBS solution. The PBS molecules with immense ionic strength and molecular weight constantly diffuse and disentangle the ZnPc polymer chains.

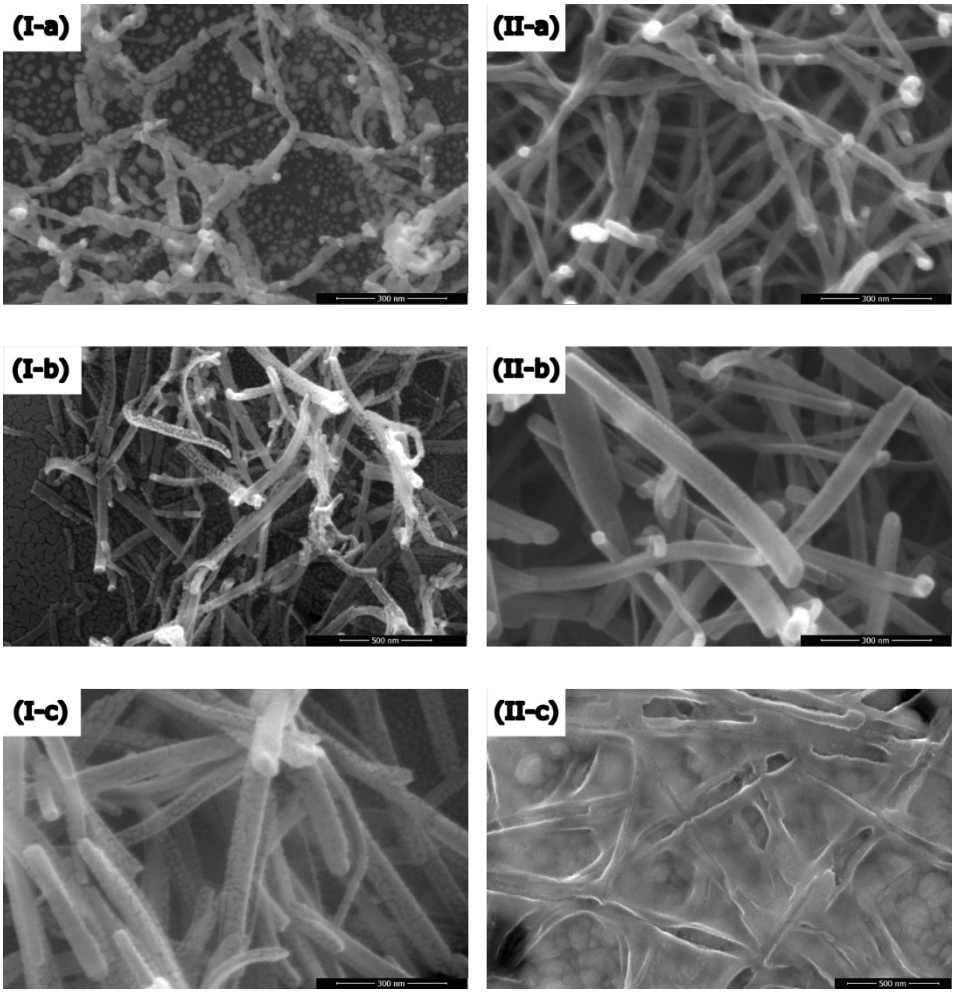

Figure 5 The morphology of ZnPc layer (I-a) injected with PBS after annealed at 100 °C, (I-b) injected with PBS after annealed at 150 °C, (I-c) injected with PBS after annealed at 220 °C; and (II-a) injected with Tris-HCl after annealed at 100 °C, (II-b) injected with Tris-HCl after annealed at 150 °C, (II-c) injected with Tris-HCl after annealed at 220 °C.

This result suggests that morphological changes are significant. Exaggerated morphological changes were observed for the samples injected with Tris-HCl buffer solution, showing the tattered fiber with embedded structures. This phenomenon can be related to the phase transformation and the interaction with the Tris-HCl.

The morphological evolutions directly affect the resonance frequency of the QCM (**Figure 6**). A sudden change of mass on the sensor's surface due to the buffer injection causes the resonance frequency of the QCM sensor to fall significantly in the first minute. The buffer molecule that is injected will then diffuse into the ZnPc layer. As a result, there is a continuous decrease in frequency during the diffusion process. The continuous reduction in the frequency of QCM resonance indicates that there has been a swelling effect on the thin layer of ZnPc due to interaction with the buffer solution.

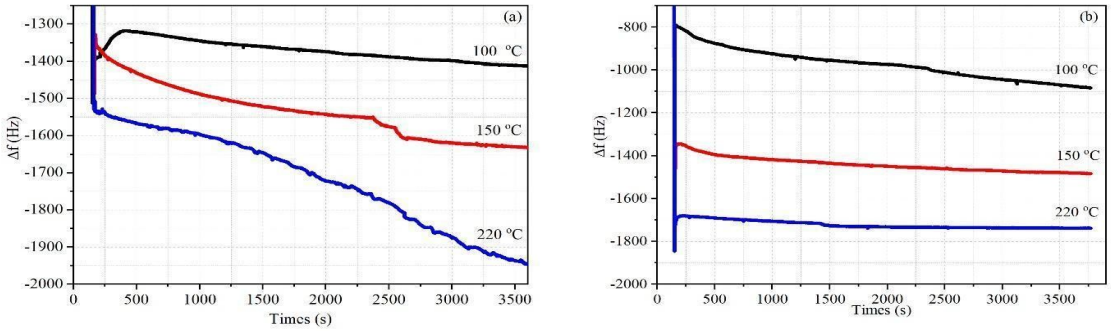

Figure 6 The QCM frequency response after the deposited ZnPc injected with (a) PBS and (b) Tris-HCl.

As shown in **Figure 6**, the annealing temperature resulted in a different trend for PBS and Tris-HCl. The trend for the PBS is steeper as the annealing increases. On the other hand, the one for the Tris-HCl is sloppier with the increase in annealing temperature. This trend demonstrates that the PBS buffer molecule diffuses and reaches saturation conditions longer than Tris-HCl. The diffusion is controlled by the analyte driving force and the ZnPc morphological restraining force. The time required by the swelling to reach saturation conditions differs depending on the amount of restrained force due to the ZnPc morphological change.

The observations show that the annealed ZnPc layer with a temperature of 220 °C has the steepest frequency change trend when injected with PBS (**Figure 6(a)**). In contrast, the Tris-HCl solution shows the sloppiest trend (**Figure 6(b)**). This change was related to the long distance between the swollen fibers. The layer has a much larger area, increasing the interaction between the buffer molecule and the ZnPc layer. In addition, due to the widening on the surface of ZnPc, which was annealed at 220 °C, the buffer molecules can more easily enter the ZnPc layer. Further observation of the data presented in **Figure 6(a)** reveals that the QCM frequency changes to the PBS injection for the layer annealed at 220 °C were gradually increased, indicating the continued diffusion of PBS molecules.

The widening of the fiber structure, the broadening distance between the fiber, and the high degree of chain mobility in the ZnPc annealed at 220 °C tend to have a smaller restrained force. The smaller force allows more diffusion of molecules. The ZnPc interacting with PBS will experience a larger frequency change than the Tris-HCl for the same treatment. However, diffusion is also affected by the ionic strength of the analyte molecules. The PBS ionic strength is higher than the Tris-HCl, providing more energy for PBS molecules to diffuse. The PBS has extra constituent ions, i.e., Na^+, K^+, and Cl^-, while the Tris-HCl only comprises Cl^- ions. In addition, the molecular weight and size of the larger PBS molecule due to phosphate ions can affect the swelling. The Phosphate ions will stretch the ZnPc chains, so more molecules can diffuse and increase the swelling effects that occur.

Evidence of the diffusion of the buffer solution in the ZnPc layer can be seen from the EDX results of the ZnPc layer after observing the swelling effect (**Figure 7**). After the swelling effect occurs, there are PBS constituent elements, as shown in **Figure 7(a)**, namely *Cl*, *Na*, and *O*, in the ZnPc layer injected with PBS buffer solution. The composition also aligns with the ZnPc layer injected with Tris-HCl buffer solution (Table 1), which found its constituent elements: *Cl*, *C*, *N*, and *O*.

Table 1 The element composition of ZnPc from EDX results.

Element of ZnPc injected with PBS	Wt%	Element of ZnPc with injected Tris-HCl	Wt%
Zn	2.61	Zn	1.69
C	81.11	C	80.79
O	10.76	O	8.55
Cl	2.37	Cl	1.22
P	1.03	N	7.75
Na	1.07	-	-
K	1.05	-	-

The PBS ionic strength, more extensive than the Tris-HCl, provides higher energy for PBS molecules to diffuse to break the ZnPc chain. In addition, due to phosphate ions, the larger PBS molecule's molecular weight and size affect the swelling. The presence of phosphate ions will stretch the ZnPc chains so that more molecules can diffuse and cause more significant swelling. The distribution of ZnPc particles after being injected with PBS and Tris-CL indicates possible changes in the particle size due to the termination process and embedded ZnPc fibers.

Conclusions

Our work showed that variation in annealing temperature from 100 to 220 °C activated gradual molecular decomposition resulting in ZnPc morphological changes. The dramatic morphological evolution started at the annealing temperature of 150 °C, where the molecular chain of the ZnPc disentangled and broke into a shorter fiber. The breaking created tapered fibers and broadened the inter-fiber space. The shortening and broadening were continued at 220 °C. The morphological changes at 220 °C were controlled by the disordering of monoclinic crystal into triclinic. The higher annealing temperature increases the frequency shift of the QCM injected with PBS and Tris-HCl solution. The different trend in frequency shift was caused by the solutions' ionic strength, which also lead to further layer transformation.

By knowing the contribution of morphological changes to the frequency response, the annealing treatment can be used to control the layer diffusion behavior. On the other hand, this work has not explained the contribution of each surface mechanism and analyte character in depth, so further studies are needed.

Acknowledgments

This work was supported by Hibah Doktor FMIPA University of Brawijaya, Indonesia, with contract numbers 3110.11/UN10.F09/PN/2022. The authors would like to Laboratorium Sentral Ilmu Hayati Universitas Brawijaya, Indonesia, (LSIH-UB) for assistance using XRD and FESEM.

References

[1] G Sauerbrey. Verwendung von schwingquarzen zur Wägung dünner schichten und zur Mikrowägung. *Zeitschrift für Physik* 1959; **155**, 206-22.

[2] M Yılmaz, M Bakhshpour, I Göktürk, AK Pişkin and A Denizli. Quartz crystal microbalance (QCM) based biosensor functionalized by HER2/neu antibody for breast cancer cell detection. *Chemosensors* 20211; **9**, 80.

[3] S Akgönüllü, E Özgür and A Denizli. Recent advances in quartz crystal microbalance biosensors based on the molecular imprinting technique for disease-related biomarkers. *Chemosensors* 2022; **10**, 106.

[4] E Haghighi and S Zeinali. Nanoporous MIL-101(Cr) as a sensing layer coated on a quartz crystal microbalance (QCM) nanosensor to detect volatile organic compounds (VOCs). *RSC Adv.* 2019; **9**, 24460-70.

[5] A Hamid, A Holloway, A Hassan and A Nabok. Investigation and analysis of Zinc phthalocyanine films for resonant gas sensor applications. *Procedia Eng.* 2016; **168**, 259-63.

[6] FI Bohrer, CN Colesniuc, J Park, ME Ruidiaz, IK Schuller, AC Kummel and WC Trogler. Comparative gas sensing in cobalt, nickel, copper, zinc, and metal-free phthalocyanine chemiresistors. *J. Am. Chem. Soc.* 2009; **131**, 478-85.

[7] L Feng, L Feng, Q Li, J Cui and J Guo. Sensitive formaldehyde detection with QCM sensor based on PAAm/MWCNTs and PVAm/MWCNTs. *ACS Omega* 2021; **6**, 14004-14.

[8] S Bhattacharjee, AA Ralib, A Vyakaranam, SD Svpk, SSS Shameem, R Sulo and AA Zainuddin. Study of multichannel QCM prospects in VOC detection. *J. Phys. Conf. Ser.* 2021; **1900**, 012020.

[9] P Izak, S Hovorka, T Bartovsky, L Bartovska and JG Crespo. Swelling of polymeric membranes in room temperature ionic liquids. *J. Membr. Sci.* 2007; **296**, 131-8.

[10] R Masruroh, MA Oktafiansyah and DJDHS Hanif. Improving the swelling effect of copper phthalocyanine surfaces by controlling surface wettability and microstructure using oxygen plasma treatment. *Rom. J. Phys.* 2022; **67**, 001.

[11] GD Francia, AI Grimaldi, E Massera, ML Miglietta and T Polichetti. Real time investigation of swelling kinetics and electrical response in polymer nanocomposite based chemical sensor. in *Procedia Chem.* 2009; **1**, 939-42.

[12] D Franke and G Gerlach. Swelling studies of porous and nonporous semi-IPN hydrogels for sensor and actuator applications. *Micromachines* 2020; **11**, 425.

[13] LA Errede. Polymer swelling: 11. A molecular interpretation of association in polystyrene-liquid systems. *Polymer* 1992; **33**, 2168-76.
[14] D Hariharan and NA Peppas. Swelling of ionic and neutral polymer networks in ionic solutions. *J. Membr. Sci.* 1993; **78**, 1-12.
[15] D Wang and CJ Cornelius. Ionomer thermodynamic interrelationships associated with wettability, surface energy, swelling, and water transport. *Eur. Polymer J.* 2016; **85**, 126-38.
[16] F Muralter, A Perrotta and AM Coclite. Thickness-dependent swelling behavior of vapor-deposited smart polymer thin films. *Macromolecules* 2018; **51**, 9692-9.
[17] S Tuntikulwattana, N Sinchaipanid, W Ketjinda, DB Williams and A Mitrevej. Fabrication of chitosanpolyacrylic acid complexes as polymeric osmogents for swellable micro/nanoporous osmotic pumps. *Drug Dev. Ind. Pharm.* 2011; **37**, 926-33.
[18] A Rianjanu, SN Hidayat, T Julian, EA Suyono, A Kusumaatmaja and K Triyana. Swelling behavior in solvent vapor sensing based on quartz crystal microbalance (QCM) coated polyacrylonitrile (PAN) nanofiber swelling behavior in solvent vapor sensing based on quartz crystal microbalance (QCM) coated polyacrylonitrile (PAN). *IOP Conf. Ser. Mater. Sci. Eng.* 2018; **367**, 012020.
[19] JD Grooth, W Ogieglo, WMD Vos, M Gironès, K Nijmeijer and NE Benes. Swelling dynamics of zwitterionic copolymers: The effects of concentration and type of anion and cation. *Eur. Polymer J.* 2014; **55**, 57-65.
[20] GB Sukhorukov, J Schmitt and G Decher. Reversible swelling of polyanion/polycation multilayer films in solutions of different ionic strength. *Berichte Bunsengesellschaft für Phys. Chem.* 1996; **100**, 948-53.
[21] AM Saeed. Temperature effect on swelling properties of commercial polyacrylic acid hydrogel beads. *Int. J. Adv. Biol. Biomed. Res.* 2013; **1**, 1614-27.
[22] M Evyapan, B Kadem, TV Basova, IV Yushina and AK Hassan. Study of the sensor response of spun metal phthalocyanine films to volatile organic vapors using surface plasmon resonance. *Sensor. Actuator. B Chem.* 2016; **236**, 605-13.
[23] EA Lukyanets and VN Nemykin. The key role of peripheral substituents in the chemistry of phthalocyanines and their analogs. *J. Porphyrins Phthalocyanines* 2010; **14**, 1-40.
[24] M Grobosch, C Schmidt, R Kraus and M Knupfer. Electronic properties of transition metal phthalocyanines: The impact of the central metal atom (d^5-d^{10}). *Org. Electron.* 2010; **11**, 1483-8.
[25] B Derkowska, M Wojdyła, R Czaplicki, W Bała and B Sahraoui. Influence of the central metal atom on the nonlinear optical properties of MPcs solutions and thin films. *Optic. Comm.* 2007; **274**, 206-12.
[26] S Senthilarasu, YB Hahn and SH Lee. Structural analysis of zinc phthalocyanine (ZnPc) thin films: X-ray diffraction study. *J. Appl. Phys.* 2007; **102**, 043512.
[27] B Przybyl and J Janczak. Complexes of zinc phthalocyanine with monoaxially coordinated imidazole-derivative ligands. *Dyes Pigments* 2016; **130**, 54-62.
[28] RL Pérez, CE Ayala, JY Park, JW Choi and IM Warner. Coating-based quartz crystal microbalance detection methods of environmentally relevant volatile organic compounds. *Chemosensors* 2021; **9**, 153.
[29] C Schünemann, C Elschner, AA Levin, M Levichkova, K Leo and M Riede. Zinc phthalocyanine - Influence of substrate temperature, film thickness, and kind of substrate on the morphology. *Thin Solid Films* 2011; **519**, 3939-45.
[30] C Medina-Plaza, G Revilla, R Muñoz, JA Fernández-Escudero, E Barajas, G Medrano, JAD Saja and ML Rodriguez-Mendez. Electronic tongue formed by sensors and biosensors containing phthalocyanines as electron mediators: Application to the analysis of red grapes. *J. Porphyrins and Phthalocyanines* 2014; **18**, 76-86.
[31] X Yang, M Zhang, Z Chen, Y Bu, X Gao, Y Sui and Y Yu. Sodium alginate micelle-encapsulating zinc phthalocyanine dye-sensitized photoelectrochemical biosensor with CdS as the photoelectric material for Hg^{2+} detection. *ACS Appl. Mater. Interfac.* 2021; **13**, 16828-36.
[32] HJ Lim, T Saha, BT Tey, WS Tan and CW Ooi. Quartz crystal microbalance-based biosensors as rapid diagnostic devices for infectious diseases. *Biosens. Bioelectron.* 2020; **168**, 112513.
[33] R Oktafiansyah, DJDH Santjojo, SP Sakti, TN Zafirah, M Ghufron, NF Khusnah and Masruroh. Swelling effect observation of the copper phthalocyanine layer on QCM and its effect on surface roughness and morphology changes. *IOP Conf. Ser. Mater. Sci. Eng.* 2020; **833**, 012082.
[34] D Roy, NM Das, N Shakti and PS Gupta. Comparative study of optical, structural and electrical properties of zinc phthalocyanine langmuir-blodgett thin film on annealing. *RSC Adv.* 2014; **4**, 42514-22.